Bond testing of salty-sand concrete reinforced with different rebars

R. Bostel[1] (iD) **, A.C.P. dos Santos[1]** (iD) **, J.B.O. Lopes[2]** (iD) **, F.L. Willrich[2]** (iD) **, R.L.O. Basso[1]** (iD) **,
M.G. Honnicke[1]** ✉ (iD)

[1] Universidade Federal da Integração Latino-Americana, Foz do Iguaçu, Brazil

[2] Itaipu Binacional, Foz do Iguaçu, Brazil

✉ marcelo.honnicke @unila.edu.br

Keywords: concrete structures, chloride-induced corrosion, bond stress, FRP, pull-out resistance

Abstract. In this work, reinforced concrete (RC) test specimens, cast with different rebars (CA-50 Steel, Basalt Fiber Reinforced Polymer – BFRP and Glass Fiber Reinforced Polymer – GFRP) and different concrete mixtures (salty-sand and unsalty sand), were submitted to the pull-out tests in order to follow the bonding behavior between the concrete and the rebar. The use of salty-sand in concrete mixtures for building construction has grown, especially in places where regular sand is scarce. However, the salinity attacks the steel rebar in RC structures, resulting in corrosion problems, which can be strongly reduced by using composite material rebars which shows, similar or superior, mechanical strength, when compared to steel rebars. Conformance testing, including X-ray powder diffraction (XPD), scanning electronic microscopy (SEM) and tensile tests, were performed on the rebars, with the aim to check the conformity of the physical, chemical and mechanical properties. Standard cylindrical test specimens (diameter of 100 mm and a height of 200 mm) and RC test specimens were prepared for compression and pull-out tests performed at 63, 217 and 315 days, after casting. The results showed a bonding loss for the RC test samples molded with CA-50 steel rebar and salty-sand concrete. On the other hand, bonding loss was not detected for test samples molded with BFRP and GFRP rebars. In conclusion, the BFRP and GFRP rebars showed to be the proper ones to be used for salty-sand concrete mixtures, however, even having higher traction resistance, their use in the RC structures will demand higher anchor lengths.

Citation: Bostel, R., dos Santos, A.C.P., Lopes, J.B.O., Willrich, F.L., Basso, R.L.O., Honnicke, M.G. Bond testing of salty-sand concrete reinforced with different rebars. Magazine of Civil Engineering. 2022. 114(6). Article No. 11407. DOI: 10.34910/MCE.114.7

1. Introduction

Long term bond testing was carried out on reinforced concrete (RC – concrete + rebar) test specimens cast with salty-sand and unsalty-sand concrete mixtures reinforced with steel and Fiber Reinforced Polymer (FRP) rebars.

RC strengths depend on the specific deformations of the rebar (steel or composite materials) and of the concrete as well as the bonding between them [1–2]. In general, the adhesion between the rebar and

concrete can be described by a chemical and a physical contribution. The last one is provided by the frictional forces arising from the roughness of the interface between the rebar and the surrounding concrete and, also, by the mechanical interlocking of the rebar surface textures [3].

The use of marine sands (salty-sand) in construction have been evaluated in different countries [4–7]. The salinity in marine sands (basically composed of sodium chloride – NaCl) attacks the steel rebars, causing corrosion problems [8] which affects the mechanical properties (and, consequently, the durability) of the RC structure. The salty-sand concrete mixtures present higher strengths at early ages compared to specimens using unsalty-sand concrete mixtures [7, 9–10]. The bonding strength decreases as the corrosion level increases [11–14]. However, for corrosion levels lower than ~ 4 %, the adhesion resistance increases proportionally to the corrosion level, which can be attributed to the deposition of oxides in the region around the rebar that increases the superficial friction [11–14]. One of the ways to evaluate the bonding between concrete and rebar, in RC, is through the pull-out tests [15] carried out on standard laboratory sample models (RC test specimens). The methodology of the pull-out test considers a tensile force applied to the rebar to pull it out of the RC concrete specimen. The pulling force permits to infer the bonding strength between concrete and rebar [16].

Fiber Reinforced Polymer (FRP) rebars [17–27] are an alternative to steel rebars in RC. They have some advantages over steel such as higher corrosion resistance, lower electrical conductivity, higher tensile strength per unit of mass and lower specific gravity [20–23].

In this work, salted and unsalted RCs cast with three different materials rebars (steel; basalt fiber rebar and; fiberglass) were comparatively investigated. The pull-out tests were performed at 63, 217 and 315 days after casting. Compressive strength tests were performed, at the same ages, in standard cylindrical salted and unsalted test specimens. The introduction of kitchen salt (sodium chloride – NaCl) into the concrete mixture had the aim to simulate the use of marine sands (salty-sand). Conformance testing, including, X-ray powder diffraction (XPD), scanning electronic microscopy (SEM) analysis (image and spectroscopy) and tensile tests, were also performed on the rebars, with the aim to check the conformity of the physical, chemical and mechanical properties of these materials.

2. Methods

2.1. Rebars conformance testing

In the process of casting the RC test specimens, rebars with three different materials were employed: i) CA-50 steel rebar; (ii) Basalt Fiber Reinforced Polymer (BFRP) rebar and; (iii) Glass Fiber Reinforced Polymer (GFRP) rebar. The physical and mechanical properties of the CA-50 steel rebars are described by the Brazilian standard ABNT NBR 7480, while the physical and mechanical properties of the composite rebars (BFRP and GFRP) are described by the Russian standard ISC GOST 31938-2012. In order to check the rebars conformance we have characterized them with few different tests: (i) X-ray powder diffraction (XPD), (ii) Scanning Electronic Microscopy (SEM) including Energy Dispersive X-ray Spectroscopy (EDS) and; (iii) tensile tests.

2.1.1. X-ray powder diffraction

The crystallographic structure of the materials employed in the different rebars was investigated by X-ray powder diffraction (XPD) measurements. They were carried out in the Bragg-Brentano geometry in a $\theta - \theta$ diffractometer (Panalytical Empyrean) by using a Cu target X-ray tube at 40 kV × 20 mA. To limit the X-ray beam area on the surface sample, 5 mm (horizontally) x 0.5 mm (vertically) crossed slits were employed. Also, in order to assure that most of the radiation is CuKα (~ 8 keV) a Ni filter was employed. Firstly, pieces (5 mm long by ~ 6 mm in diameter) of the different rebar types (CA-50 steel, BFRP and GFRP) were prepared in a home-made cold mounting resin for the XPD measurements. To further characterize the FRP rebars we decided to grind them until get a homogeneous powder (particle size between 1 μm and 6 μm) and repeat the XPD measurements.

2.1.2. Scanning electron microscopy

The scanning electronic microscopy (SEM) measurements [including energy dispersive X-ray spectroscopy (EDS)] were carried out with a Zeiss EVO MA10 electronic microscope. Again, cross section pieces (5 mm long by ~ 6 mm in diameter) of the different rebar types (CA-50 steel, BFRP and GFRP) were prepared. Also, in order to try to measure only the fibers and not only the FRP resins, longitudinal section pieces (5 mm long) were also prepared. In the process of cutting the different FRP section pieces, one BFRP rebar sample was unraveled, showing up the basalt fibers. This sample was also used for the SEM images. The sectioned samples were lapped and polished. All the samples (sections and the unraveled) were cleaned with isopropanol and then coated, by sputtering deposition, with palladium (Pd) for the SEM analysis. The samples were then mounted in the SEM reel table.

2.1.3. Tensile tests

In order to confirm compliance with the specifications and standards, the different rebar types (CA-50 steel, BFRP and GFRP) were also submitted to tensile tests. The tests were performed in an universal testing machine (TimeGroup WAW1000C). The operation of the universal testing machine is made by a software that acquires the loading data as function of time. For consistency check, the tests, carried out with the CA-50 steel rebars, were also measured with a strain gauge (displacement indicator), attached to the test machine.

2.2. Concrete specimens design and preparation

Standard cylindrical test specimens (diameter of 100 mm and a height of 200 mm), for compression tests, and RC test specimens, for pull-out tests, were prepared. The procedure for assembling the RC test specimens and for executing the pull-out tests are reported in the ASTM standard C234-91a. In this work, the RC test specimens were cast in standard cylindrical molds (diameter of 150 mm and a height of 300 mm) however, slightly modified, by inserting a small cylindrical section, set on the top of the RC test specimens, as described in a previous work [28]. The small cylindrical section was included in the mold in order to reduce the RC test specimens thickness to be able to carry out in-situ X-ray inspection during the pull-out tests [28]. Nevertheless, this methodology did not showed to be efficient for RC test specimens with BFRP and GFRP rebars since the density of the rebars are very close to the concrete density then producing no contrast in the acquired in-situ X-ray images. To solve this problem, in-situ phase contrast X-ray inspection [29] is envisaged. The challenge is to mount such an experiment in the universal testing machine especially due to the size of the radiation shielding, since the sample to detector distance needs to be increased to ~ 1 m.

Coming back to the RC test specimens design, the bonding embedment length (anchorage length) between the concrete and the rebars (CA-50 steel, BFRP and GFRP) was kept to a length of 70 mm on the longitudinal axis, including the section with the reduced diameter. In order to avoid contact between the concrete and the steel rebar along the remaining length (180 mm), a flexible polyvinyl chloride tube with an internal diameter of 8 mm was placed around the rebar and sealed at the ends with ethylene vinyl acetate glue.

Normal (unsalty-sand) and salty-sand concrete mixtures (Table 1) were made up with Portland cement with a high initial strength (Ciplan CPV Extra Forte). The salty-sand concrete mixtures were prepared with unsalted sand, however, adding kitchen salt (sodium chloride – NaCl) to the mixture with the same salt concentration of sea sands reported in the literature [23]. All the concrete mixtures were prepared in order to have an initial compressive strength of 30 MPa (theoretically estimated). The slump test (in accordance with the Brazilian standard ABNT NBR NM 67), measured just before casting the test specimens, was found to be in the range of 35 mm to 75 mm for unsalty-sand concrete mixtures and in the range of 55 mm to 160 mm for the salty-sand concrete mixtures. The sand comes from regional natural river extraction (Foz do Iguacu, Brazil) and the coarse aggregate is made from the basaltic rock. Both are in accordance with the Brazilian standard ABNT NBR 7211, i.e., maximum diameters of 2.4 mm (sand) and 9.5 mm (coarse aggregate).

Table 1. Concrete mixture specifications used for casting the RC test specimens (pull-out tests) and the standard cylindrical test specimens (compression tests) for a theoretically estimated compressive strength value of 30 MPa

Material	Unsalty-sand concrete mixture mass (kg)	Salty-sand concrete mixture mass (kg)
Cement	25.50	25.50
Sand	74.97	74.97
Gravel	85.00	85.00
Water	17.00	17.00
Salt	–	0.4335

The water was provided by the local water supply company (Sanepar). The concrete was mixed in an electric mixer with a capacity of 300 l. 72 RC test specimens were cast for each different rebar type (CA-50 steel, BFRP and GFRP) in two different dozen sets (unsalty-sand and salty-sand concrete mixtures) (Fig. 1 and Table 2). As previously mentioned, at the same time, standard cylindrical test specimens (72 in total with a diameter of 100 mm and a height of 200 mm), one dozen for each different set, were also cast (Fig. 1 and Table 2). The aim to do that is to carry out compression tests and pull-out tests at the same time in order to determine both, the concrete compressive strength and the bond strength. For the RC test specimens, the concrete was cast in four layers. The first layer filled the 35 mm diameter region. The other

three layers were equally divided along the height of the specimen. For the standard cylindrical test specimens the concrete was cast in tree layers of ranging from ~ 60 mm to ~ 70 mm each. For the concrete compaction; the specimens were repeatedly tamped (25 times for each layer, in accordance with the Brazilian standard ABNT NBR 5738), using a metal rod to avoid the formation of large voids and aggregate segregations inside the specimen. The specimens were demolded 48 h after casting and were placed in a humid chamber until the test dates.
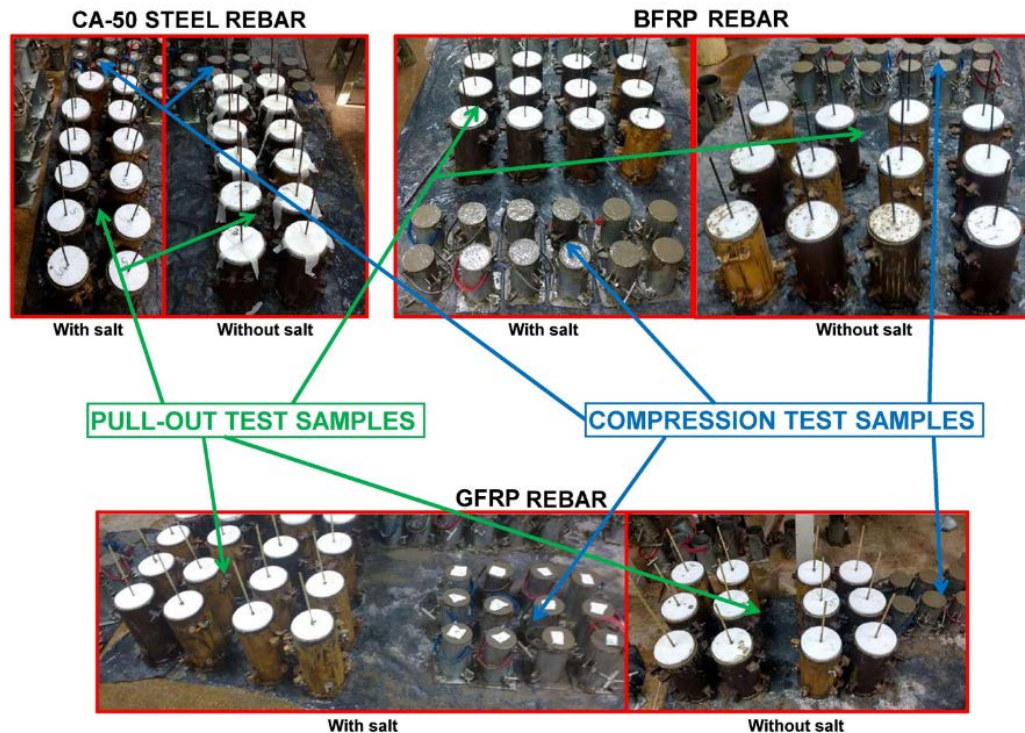

Figure 1. Cast samples for the pull-out (Reinforce Concrete – RC test specimens) and compression tests (standard cylindrical test specimens). Salty-sand and unsalty-sand samples and unsalted samples.

Table 2. RC test specimens (pull-out tests) and the standard cylindrical test specimens (compression tests) inventory

Rebar type	Unsalty-sand RC test specimens (unit)	Salty-sand RC test specimens (unit)	Unsaly-sand standard cylindrical test specimens (unit)	Salty-sand standard cylindrical test specimens (unit)
Steel	12	12	12	12
BFR	12	12	12	12
GFR	12	12	12	12

2.3. Pull-out and compression tests

The pull-out tests on the RC test specimens and the compression tests on the standard cylindrical test specimens were carried out at the universal testing machine (TimeGroup WAW1000C) at 63, 217 and 315 days after casting. For the pull-out tests (Fig. 2) we have designed a metal cradle (carbon steel) for holding the RC test specimens, as described in a previous work [28]. Two different concrete mixtures (unsalty-sand and salty-sand) and three different rebar types (CA-50 steel, BFRP and GFRP) were studied.
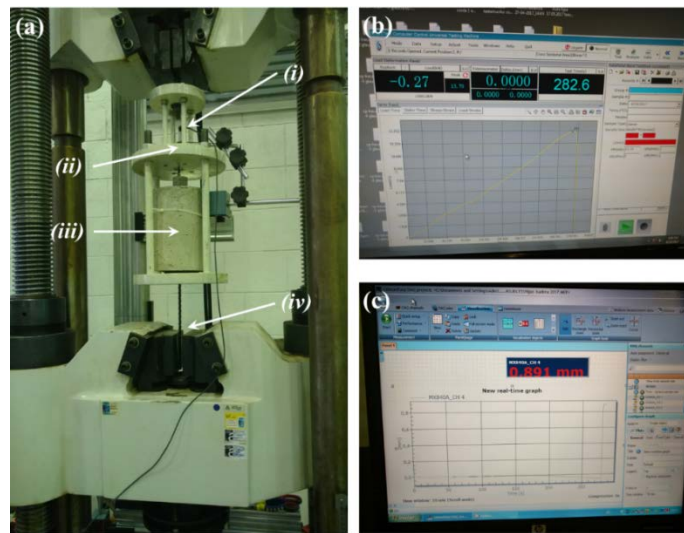
**Figure 2. (a) Setup for the pull-out test mounted on the universal testing machine:
(i) Displacement indicator; (ii) Metallic cradle; (iii) Reinforced concrete (RC) test specimen and;
(iv) Detail of the rebar (in this a BFRP) fixed in the universal testing machine clamps.
(b) Picture of the computer screen showing the software that controls the operation
of the machine and stores the loading data versus time. (c) Picture of the computer screen
showing the software that stores the displacement versus time data, as measured
by the displacement indicator.**

3.   Results and Discussion

3.1. Conformance testing

For the CA-50 steel rebar the XPD results (represented by the diffractogram in Fig. 3) show the main X-ray diffraction peaks of 0.95Fe0.05Mn alloy (indexed by JCPDS no. 98-010-3521), as expected. Also, X-ray diffraction peaks of the cold mounting resin were detected. For the XPD measurements carried out on the BFRP and on the GFRP rebars, only the cold mounting resin X-ray diffraction peaks were found (results not presented here). For this reason, the FRP rebars were grind and further characterized by XPD.

For the grind FRP rebars, few X-ray diffraction peaks were found and they look similar (same angular position) for both samples (BFRP and GFRP) (Fig. 4). Since the diffraction peaks are angularly broad, which is characteristic of low range cristallinity materials (such as paraffin wax, polypropylene, etc.) [30, 31], we attributed them to the FRP resins. However, we were not able to get the diffractogram indexed. Then, at last, we decided to proceed with spectroscopy analysis in order to check the main components (chemical elements) of each FRP rebar. This was made by scanning electronic microscopy (SEM) including energy dispersive X-ray spectroscopy (EDS).
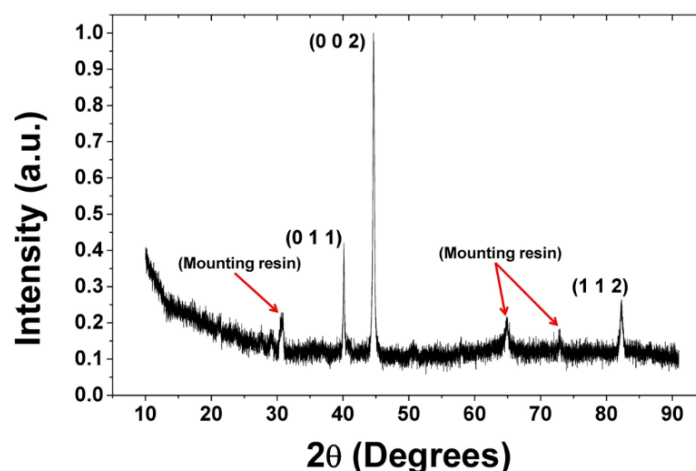

**Figure 3. Diffractogram for the CA-50 steel rebar. The three main diffraction peaks were indexed
to be 0.95Fe0.05Mn alloy (JCPDS no. 98-010-3521). Each diffraction peak represents the X-ray
diffraction by a different crystallographic plane, indicated between the brackets,
by the Miller indices. Diffraction peaks of the mounting resin are also present.**
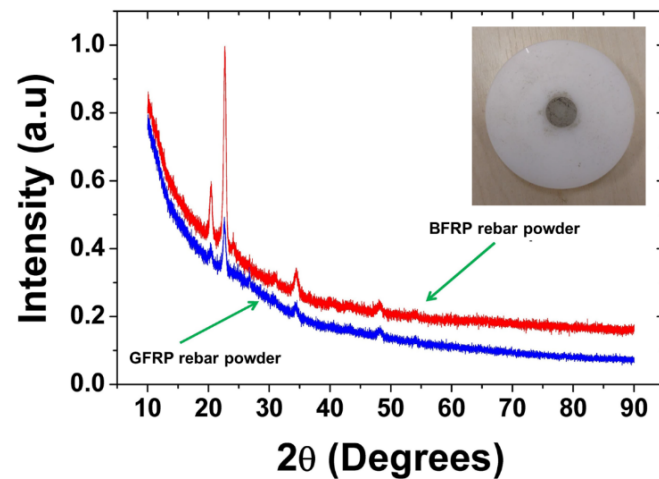
Figure 4. Diffractograms of the BFRP and GFRP rebar powders. As an example, in the inset, is shown the GFRP powder prepared in a polyamide sample holder for the XPD measurements.

The SEM images of the basalt fiber and the glass fiber themselves, are shown Fig. 5. Diameter sizes of 17 μm and 18 μm, respectively, were measured. In Fig. 6 and 7 are shown the EDS analysis for the different sections of BFRP and GFRP, respectively. The results show the presence of oxygen (O), silicon (Si), iron (Fe), calcium (Ca), magnesium (Mg), sodium (Na) and potassium (K) for the BFRP fibers and; oxygen (O), silicon (Si), calcium (Ca) and aluminum (Al) for the GFRP fibers, in accordance with other data presented in the literature [32]. Some measurements show also the presence of carbon (C), gold (Au) and palladium (Pd). The first occurs because some of the measured fibers can still be embedded in the FRP resin. Au and Pd are present as a consequence of the coating material used for SEM analysis. In some results they were electronically filtered and did not showed up.
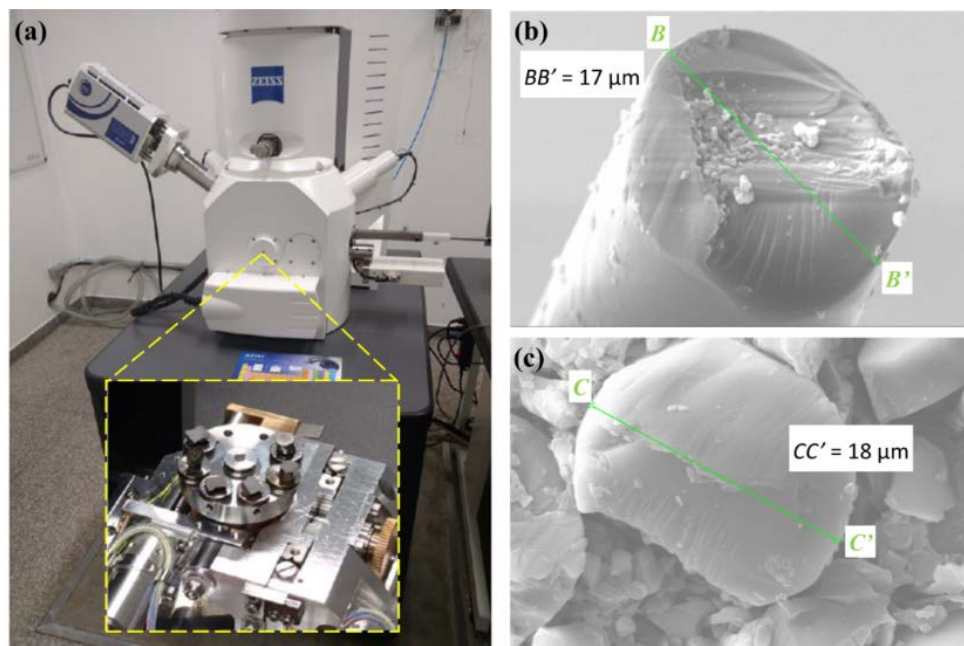

Figure 5. (a) Scanning electron microscope (SEM). In the inset it is shown, mounted in the reel table, inside the SEM vacuum chamber, all the samples (sectioned FRP and the unraveled sample) already coated with palladium. (b) SEM image of the basalt fiber. (c) SEM image of the glass fiber.
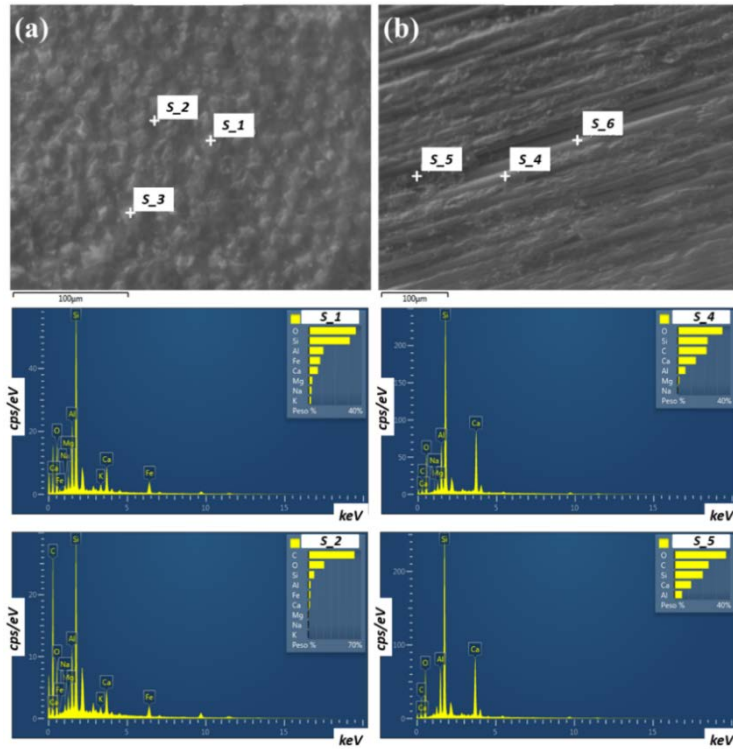
Figure 6. SEM / Energy Dispersive X-ray Spectroscopy (EDS) measurements on the sections of the BFRP rebar. (a) Cross section and (b) Longitudinal section. Results on the different points where de EDS was performed were chosen to show here: s1, s2, s4 and s5. They correspond to areas with the fiber (s1 and s4) and areas with FRP resin (s2 and s4). Carbon (C) was also present in the s4 area, indicating that the basalt fiber is still embedded in the FRP resin.
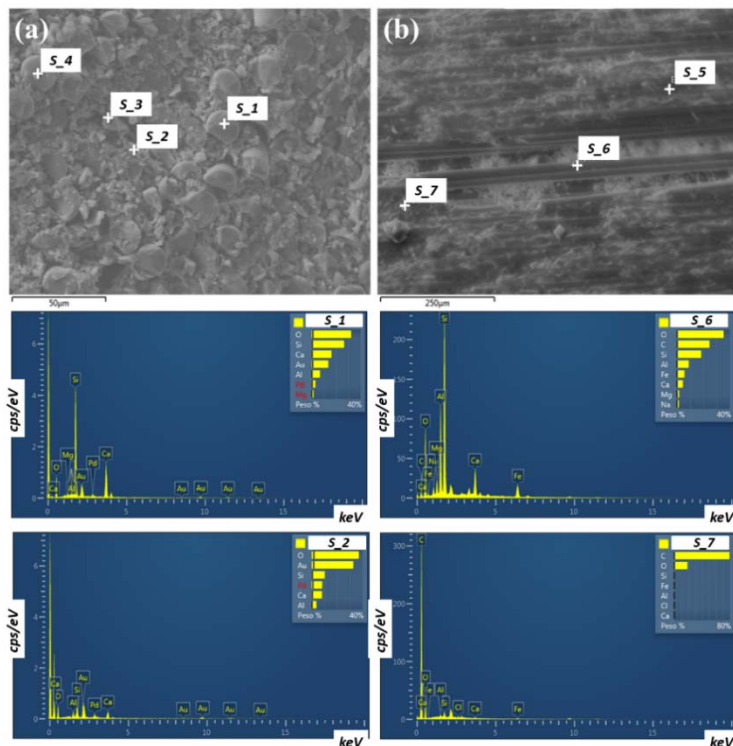
Figure 7. SEM / EDS measurements on the sections of the GFRP rebar. (a) Cross section and (b) Longitudinal section. Results on the different points where de EDS was performed were chosen to show here: s1, s2, s6 and s7. They correspond to areas with the fiber (s1 and s4) and, in principle, areas with FRP resin (s2 and s7). Gold (Au) and Palladium (Pd), not electronically filtered in these measurements, were found in s1 and s2. Carbon (C) was not found in s2, indicating that there is no FRP resin in that area. However, Carbon (C) was in the s6 area, indicating that the glass fiber is still embedded in the FRP resin.

The tensile test results for the CA-50 steel rebars are presented in Fig. 8. For the BFRP and GFRP rebars, firstly, they were fixed as the CA-50 steel rebars, i.e, directly to the clamps of the universal testing machine [Fig. 9(a) and 9(b)]. This methodology was not the most appropriate due to the characteristics of BFRP and GFRP rebars. When the applied load increases, a slippage occurs in the contact region between the rebars and the clamps even before reaching the yield strength limit. This damaged the tested rebars [Fig. 9(c)]. To solve this problem, the rebars extremities were embedded in resin-filled (in our case, polyester putty) steel tubes (sleeves) [Fig. 9(d)] in a methodology similar to the recommended by the Russian standard ISC GOST 31938-2012. Using such a methodology, the universal testing machine clamps will be in contact with the steel tubes (sleeves) and not in direct contact with the rebars, thus preventing the rebars slippage in the clamps region when pulled. As an example, Fig. 9(e) shows a GFPR rebar with the resin filled steel tubes mounted in the universal testing machine previously to the tensile test. Even with that, the tests showed to be unsuccessful, because, during load application, the steel tube (sleeve) was crushed, most probably, due to some void inside the steel tube. This leads to a loss of adhesion between the hardened resin and the steel tube. Consequently, the rebars, together with the hardened resin, were torn out from the steel tube, thus not allowing the test to be completed. However, the rebar manufacturer (Composite Chelyabinsk Group LLC) indicates that the tensile strength of both BFPR rebar and GFPR rebar is ~ 1000 MPa. In the case of the rebar used in this work, which have diameter of 6 mm, this is equivalent to a maximum force of 28.3 KN. In pull-out tests that will be further presented, the maximum applied force never exceeded 20 KN, which safely moves away from possibility of breaking off the BRPR and GRPR rebars before reaching the ultimate bonding strength.
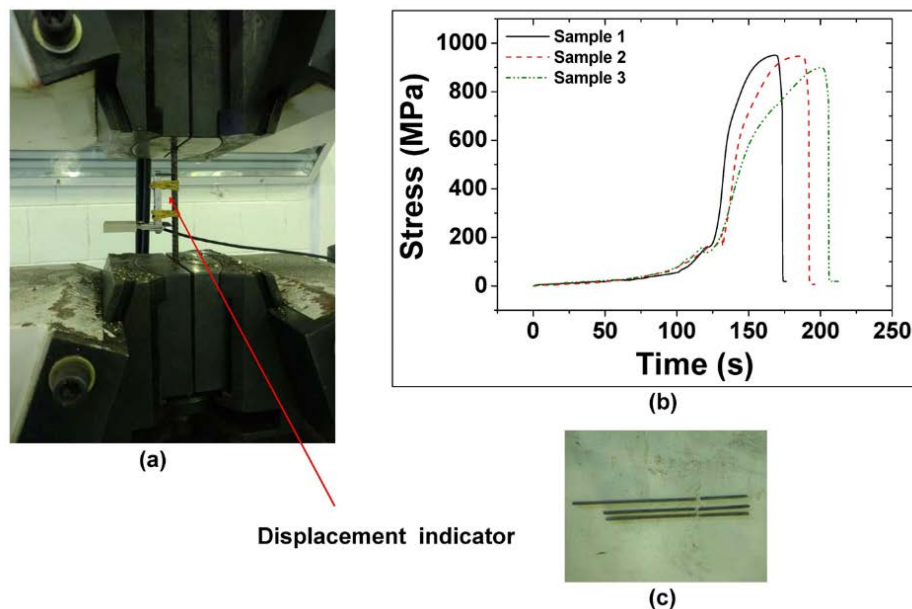
Figure 8. Tensile tests for the CA-50 steel rebar. (a) CA-50 Steel rebar fixed in the clamps of the universal testing machine. Use of strain gauge (displacement indicator) installed in contact with CA-50 steel rebar. (b) Stress (MPa) x time (s) results for the three different the CA-50 steel rebar samples. (c) CA-50 steel rebar samples after the tensile test.
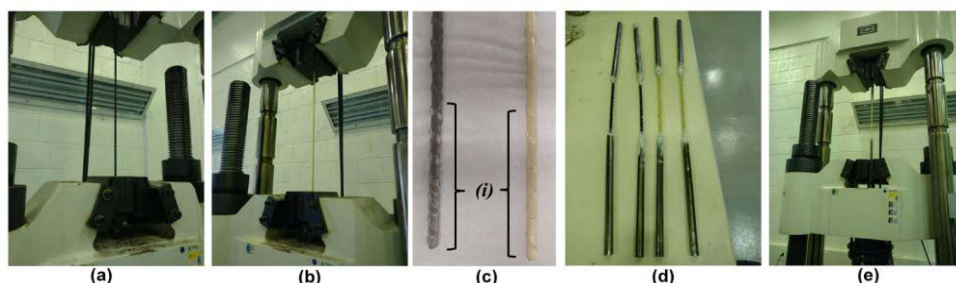
Figure 9. Tensile tests for the FRP rebars. BFRP rebar (a) and GFRP rebar (b) directly fixed into the clamps of the universal testing machine. (c) BFRP rebar (left) and GFRP rebar (right) after tensile tests showing the damage in the rebars (i) due to the slipping in the universal testing machine clamps. (d) Samples of BFRP rebar (left) and GFRP rebar (right) embedded in resin filled steel tubes (sleeves). (e) GFRP rebar with the resin filled steel tubes mounted in the universal testing machine for the tensile test.

3.2. Compression and bond strengths

The results are summarized in Tables 3-14. A total of 18 sets of pull-out tests were carried out on 36 RC test specimens and a total of 18 sets of compression tests were done on 60 standard cylindrical test samples. The results for the average bond strength values (acquired with the pull-out tests) for the different rebar types with different concrete mixtures at different ages (Tables 3, 5, 7, 9, 11 and 13), for better comparison, are summarized in the Fig. 10, 11 and 12.

Table 3. Results for the pull-out tests on unsalty-sand RC test specimens with CA-50 steel rebar.

Specimen #	Time after molding (days)	Bond strength (MPa)	
		Per specimen	Average
POT-AC-SS-01	63	19.24	18.10
POT-AC-SS-02		16.96	
POT-AC-SS-03	217	16.21	16.47
POT-AC-SS-04		16.74	
POT-AC-SS-05	315	18.87	19.06
POT-AC-SS-06		19.25	

Table 4. Results for the compression tests on the unsalty-sand standard cylindrical test specimens molded at the same time with the unsalty-sand RC test specimens with CA-50 steel rebar. The result for the specimen RC-AC-SS-04 was excluded since its value is 5% (or more) greater than the average.

Specimen #	Time after molding (days)	Compressive strength (MPa)	
		Per specimen	Average
RC-AC-SS-01	63	33.10	33.16
RC-AC-SS-02		33.25	
RC-AC-SS-03		33.12	
RC-AC-SS-04		~~36.47~~	
RC-AC-SS-05	217	43.00	42.63
RC-AC-SS-06		41.96	
RC-AC-SS-07		41.92	
RC-AC-SS-08		43.62	
RC-AC-SS-09	315	40.20	42.13
RC-AC-SS-10		44.05	

Table 5. Results for the pull-out tests on salty-sand RC test specimens with CA-50 steel rebar.

Specimen #	Time after molding (days)	Bond strength (MPa)	
		Per specimen	Average
POT-AC-CS-01	63	18.93	17.99
POT-AC-CS-02		17.06	
POT-AC-CS-03	217	15.30	15.69
POT-AC-CS-04		16.08	
POT-AC-CS-05	315	14.23	14.00
POT-AC-CS-06		13.77	

For the RC test specimens with CA-50 steel rebars and salty-sand concrete mixtures there is a reduction in the bond strength along the time (~ 20 % when comparing to the measured bond strengths in 315 days and 63 days and ~ 26 % when compared with the RC test specimens with CA-50 steel rebars and unsalty-sand concrete mixture) (Fig. 10, Table 3 and 5). This can be attributed to the initial corrosion stages in the CA-50 steel rebars due to the higher salinity of the concrete mixture.

For the RC tests specimens with BFRP rebars and unsalty-sand concrete mixture, there is a reduction in the bond strength along the time (Fig. 11, Table 7). However, since this difference, at 315 days, is only 9 % for the specimens with different concrete mixtures (salty-sand an unsalty-sand), one can say that, within the error bars, the bond strengths are, approximately, the same. On the other hand, for the RC test specimens with BFRP rebars and salty-sand concrete mixtures there is an increase in the bond strength along the time (Fig. 11, Table 9), this can be related to the hydration of the cementitious matrix, reflected on the higher compressive strength (Table 10).

Table 6. Results for the compression tests on the salty-sand standard cylindrical test specimens molded at the same time with the salty-sand RC test specimens with CA-50 steel rebar. The result for the specimen RC-AC-CS-08 was excluded since its value is 5% (or more) smaller than the average.

Specimen #	Time after molding (days)	Compressive strength (MPa)	
		Per specimen	Average
RC-AC-CS-01	63	35.74	35.68
RC-AC-CS-02		35.62	
RC-AC-CS-03		34.97	
RC-AC-CS-04		36.37	
RC-AC-CS-05	217	39.56	39.58
RC-AC-CS-06		40.11	
RC-AC-CS-07		39.06	
RC-AC-CS-08		~~35.71~~	
RC-AC-CS-09	315	42.06	42.50
RC-AC-CS-10		42.94	

Figure 10. Temporal evolution of the average bond strength values for the RC test specimens with CA-50 steel rebars with different concrete mixtures (salty-sand and unsalty-sand). The error bars are the standard deviations.

Table 7. Results for the pull-out tests on unsalty-sand RC test specimens with BFRP rebar. The result for the specimen POT-FB-SS-01 was discarded due to an slippage of the BFRP rebar in the clamps of universal testing machine. The slippage occurred before the maximum bond strength between the BFRP rebar and the concrete.

Specimen #	Time after molding (days)	Bond strength (MPa)	
		Per specimen	Average
POT-FB-SS-01	63	10.38	14.33
POT-FB-SS-02		14.33	
POT-FB-SS-03	217	15.10	15.13
POT-FB-SS-04		15.16	
POT-FB-SS-05	315	12.36	12.78
POT-FB-SS-06		13.19	

Table 8. Results for the compression tests on the unsalty-sand standard cylindrical test specimens molded at the same time with the unsalty-sand RC test specimens with BFRP rebar.

Specimens #	Time after molding (days)	Compressive strength (MPa)	
		Per specimen	Average
RC-FB-SS-01	63	27.20	27.34
RC-FB-SS-02		26.75	
RC-FB-SS-03		26.63	
RC-FB-SS-04		28.78	
RC-FB-SS-05	217	36.37	36.74
RC-FB-SS-06		36.97	
RC-FB-SS-07		36.92	
RC-FB-SS-08		36.70	
RC-FB-SS-09	315	29.73	30.05
RC-FB-SS-10		30.38	

Table 9. Results for the pull-out tests on salty-sand RC test specimens with BFRP rebar

Specimen #	Time after molding (days)	Bond strength (MPa)	
		Per specimen	Average
POT-FB-CS-01	63	12.39	12.33
POT-FB-CS-02		12.27	
POT-FB-CS-03	217	12.83	13.33
POT-FB-CS-04		13.84	
POT-FB-CS-05	315	12.87	14.04
POT-FB-CS-06		15.21	

Table 10. Results for the compression tests on the salty-sand compression test specimens molded at the same time with the salty-sand RC test specimens with BFRP steel rebar. The result for the specimen RC-FB-CS-08 was excluded since its value is 5% (or more) smaller than the average.

Specimen #	Time after molding (days)	Compressive strength (MPa)	
		Per specimen	Average
RC-FB-CS-01	63	32.05	31.80
RC-FB-CS-02		31.50	
RC-FB-CS-03		32.63	
RC-FB-CS-04		31.03	
RC-FB-CS-05	217	36.65	37.20
RC-FB-CS-06		37.40	
RC-FB-CS-07		37.57	
RC-FB-CS-08		~~31.33~~	
RC-FB-CS-09	315	33.97	33.74
RC-FB-CS-10		33.50	

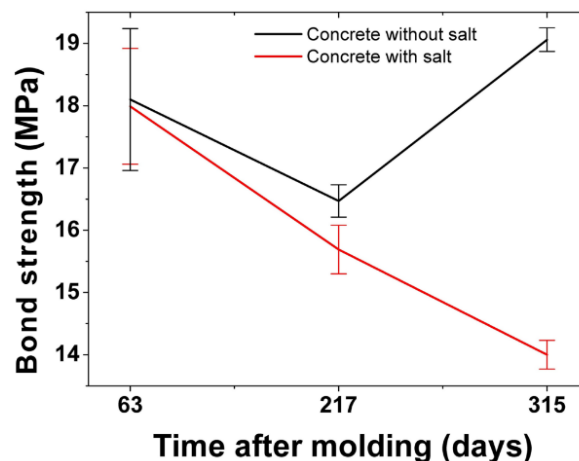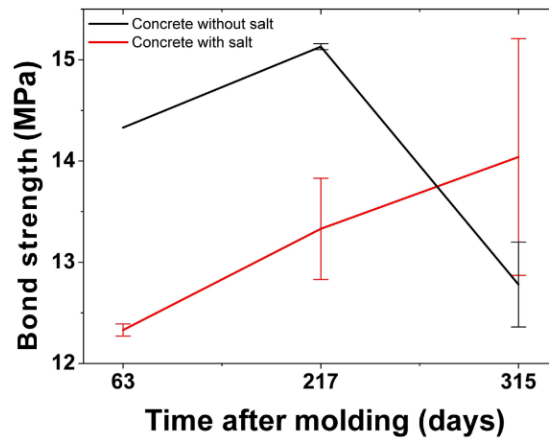**Figure 11. Temporal evolution of the average bond strength values for the RC test specimens with BFRP rebars with different concrete mixtures (salty-sand and unsalty-sand). The error bars are the standard deviations.**

For the RC test specimens with GFRP rebars the measured bond strengths, for all the concrete mixtures (salty-sand and unsalty-sand) and all the ages, were very similar (Fig. 12, Table 11 and 13).

In summary, the bond strength results showed that BFRP and GFRP rebars can be successfully used in salty-sand concrete mixtures. However, the BFRP and GFRP rebars showed, in all the reported measurements (Table 3, 5, 7, 9, 11, 13 and Fig. 10–12), bond strengths smaller than the bond strengths for the CA-50 steel rebars. Then, even the BFRP and GFRP rebars having higher tensile strength than the CA-50 steel rebar, their use in the RC structures will demand higher anchorage lengths, as already reported in the literature [3, 33]. This is attributed to the difference in the surface deformations of the FRP rebars and steel rebar [33].

Table 11. Results for the pull-out tests on unsalty-sand RC test specimens with GFRP rebar.

Specimen #	Time after molding (days)	Bond strength (MPa)	
		Per specimen	Average
POT-FV-SS-01	63	13.20	14.50
POT-FV-SS-02		15.79	
POT-FV-SS-03	217	12.56	12.43
POT-FV-SS-04		12.30	
POT-FV-SS-05	315	13.63	12.95
POT-FV-SS-06		12.26	

Table 12. Results for the compression tests on the unsalty-sand standard cylindrical test specimens molded at the same time with the unsalty-sand RC test specimens with GFRP rebar.

Specimen #	Time after molding (days)	Compressive strength (MPa)	
		Per specimen	Average
RC-FV-SS-01	63	35.87	36.27
RC-FV-SS-02		36.20	
RC-FV-SS-03		36.75	
RC-FV-SS-04		36.27	
RC-FV-SS-05	217	42.09	41.74
RC-FV-SS-06		40.87	
RC-FV-SS-07		42.92	
RC-FV-SS-08		41.09	
RC-FV-SS-09	315	41.09	41.99
RC-FV-SS-10		42.89	

Table 13. Results for the pull-out tests on salty-sand RC test specimens with GFRP rebar. The result for the specimen POT-FV-CS-04 was discarded due to a crack in the in the small cylindrical section during to the pull-out test which prevented us to determine the bond strength between GFRP rebar and the concrete.

Specimen #	Time after molding (days)	Bond strength (MPa)	
		Per specimen	Average
POT-FV-CS-01	63	15.18	14.68
POT-FV-CS-02		14.19	
POT-FV-CS-03	217	13.95	13.95
POT-FV-CS-04		~~9.23~~	
POT-FV-CS-05	315	14.07	12.71
POT-FV-CS-06		11.35	

Table 14. Results for the compression tests on the salty-sand standard cylindrical test specimens molded at the same time with the salty-sand RC test specimens with GFRP steel rebar.

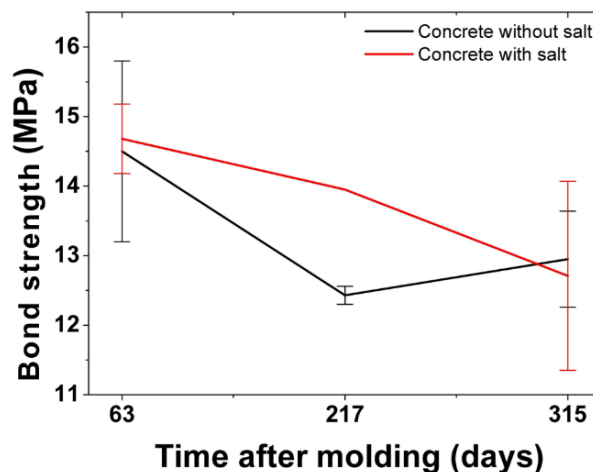| Specimen #	Time after molding (days)	Compressive strength (MPa)	
		Per specimen	Average
RC-FV-CS-01	63	37.27	37.10
RC-FV-CS-02		36.85	
RC-FV-CS-03		36.32	
RC-FV-CS-04		37.95	
RC-FV-CS-05		41.67	
RC-FV-CS-06	217	42.37	42.35
RC-FV-CS-07		42.24	
RC-FV-CS-08		43.12	
RC-FV-CS-09	315	40.89	39.87
RC-FV-CS-10		38.85	

Figure 12. Temporal evolution of the average bond strength values for the RC test specimens with GFRP rebars. with different concrete mixtures (salty-sand and unsalty-sand). The error bars are the standard deviations.

4. Conclusion

Long term pull-out tests were carried out in Reinforced Concrete (RC) test specimens with CA-50 steel rebars, Basalt Fiber Reinforced Polymer (BFRP) rebars and Glass Fiber Reinforce Polymer (GFRP) rebars with salty-sand and unsalty-sand concrete mixtures. For different ages (up to 315 days after casting) pull-out tests and compression tests were performed. Conformance testing, including X-ray powder

diffraction (XPD), Scanning Electronic Microscopy (SEM) and tensile tests, were carried out on the rebars previously to the pull-out and compression tests.

Our results showed that all the tested RC test specimens cast with different rebar types (CA-50 steel, BFRP and GFRP) and unsalty-sand concrete mixtures did not show expressive changes in the measured bond strengths along the time. However, for the RC test specimens cast with salty-sand concrete mixtures, the results were different. For the RC test specimens molded with BFRP and GFRP rebars also no expressive changes in the measured bond strengths along the time were found. Although for the RC test specimens cast with CA-50 steel rebars, a reduction in the bond strength along the time was detected (~20 % when comparing the measured strengths in 315 days and 63 days and 26 % when compared with the RC test specimens with CA-50 steel rebars and unsalty-sand concrete mixture). This can be attributed to the initial corrosion stages in the CA-50 steel rebars (not detected in the BFRP and GFRP rebars) due to the higher salinity of the concrete mixtures.

At last, the BFRP and GFRP rebars showed to be the proper rebars to be used for salty-sand concrete mixtures. However, since their bond strengths are smaller than the bond strengths for the CA-50 steel rebars in all the reported measurements, their use in the RC structures, will demand higher anchor lengths even having higher traction resistance.

References

1. Fanella, D.A. Reinforced Concrete Structures: Analysis and Design. 1st ed. New York, McGraw-Hill, 2010. 652 p.
2. Wight, J., Macgregor, J. Reinforced Concrete: Mechanics and Design: International Edition. New Jersey, Pearson Education, 2012. 1176 p.
3. Quayyum, S. Bond behaviour of Fibre Reinforced Polymer (FRP) rebars in concrete. University of British Columbia, 2010. 190 p.
4. Yin, H., Li, Y., Lv, H., Gao, Q. Durability of sea-sand containing concrete: Effects of chloride ion penetration. Mining Science and Technology. 2011. 21 (1). Pp. 123–127. DOI: 10.1016/j.mstc.2010.07.003
5. Apostolopoulos, C.A., Demis, S., Papadakis, V.G. Chloride-induced corrosion of steel reinforcement - Mechanical performance and pit depth analysis. Construction and Building Materials. 2013. 38. Pp. 139–146. DOI: 10.1016/j.conbuildmat.2012.07.087
6. Kog, Y.C. High-performance concrete made with dune sand. Magazine of Concrete Research. 2020. 72 (20). Pp. 1036–1046. DOI: 10.1680/jmacr.18.00073
7. Wegian, F.M. Effect of seawater for mixing and curing on structural concrete. The IES Journal Part A: Civil & Structural Engineering. 2010. 3 (4). Pp. 235–243. DOI: 10.1080/19373260.2010.521048
8. Tuutti, K. Corrosion of steel in concrete. Swedish Cement and Concrete Research Institute, 1982. 468 p.
9. Olutoge, F.A., Amusan G.M. The Effect of Sea Water on Compressive Strength of Concrete. International Journal of Engineering Science Invention. 2014. 3 (7). Pp. 23–31.
10. Nagabhushana, D.R., Hebbal, D., Akash, N., Deepak, S., Kumar, M. Effect of salt water on compressive strehgth of concrete. International Research Journal of Engineering and Technology. 2017. 4 (5). Pp. 2687–2690.
11. Fang, C., Lundgren, K., Chen, L., Zhu, C. Corrosion influence on bond in reinforced concrete. Cement and Concrete Research. 2004. 34 (11). Pp. 2159–2167. DOI: 10.1016/j.cemconres.2004.04.006
12. Fang, C., Lundgren, K., Plos, M., Gylltoft, K. Bond behaviour of corroded reinforcing steel bars in concrete. Cement and Concrete Research. 2006. 36 (10). Pp. 1931–1938. DOI: 10.1016/j.cemconres.2006.05.008
13. Lundgren, K. Effect of corrosion on the bond between steel and concrete: an overview. Magazine of Concrete Research. 2007. 59 (6). Pp. 447–461. DOI: 10.1680/macr.2007.59.6.447
14. Yalciner, H., Eren, O., Sensoy, S. An experimental study on the bond strength between reinforcement bars and concrete as a function of concrete cover, strength and corrosion level. Cement and Concrete Research. 2012. 42 (5). Pp. 643–655. DOI: 10.1016/j.cemconres.2012.01.003
15. Watstein, D. Bond Stress in Concrete Pullout Specimens. ACI Journal Proceedings. 1941. 38. Pp. 37–52. DOI: 10.14359/8586
16. Nawy, E.G. Reinforced Concrete: a Fundamental Approach. New Jersey, Pearson, 2008. 944 p.
17. Teng, J.G., Chen, J.F., Smith, S.T., Lam, L. Behaviour and strength of FRP-strengthened RC structures: a state-of-the-art review. Proceedings of the Institution of Civil Engineers – Structures and Buildings. 2003. 156 (1). Pp. 51–62. DOI: 10.1680/stbu.2003.156.1.51
18. Yuan, H., Teng, J.G., Seracino, R., Wu, Z.S., Yao, J. Full-range behavior of FRP-to-concrete bonded joints. Engineering Structures. 2004. 26 (5). Pp. 553–565. DOI: 10.1016/j.engstruct.2003.11.006
19. Okelo, R., Yuan, R.L. Bond Strength of Fiber Reinforced Polymer Rebars in Normal Strength Concrete. Journal of Composites for Construction. 2005. 9 (3). Pp. 203–213. DOI: 10.1061/(ASCE)1090-0268(2005)9:3(203)
20. Karbhari, V.M. Durability of Composites for Civil Structural Applications. Pennsylvania, Woodhead Publishing, 2007. 944 p.
21. Lau, D., Pam, H.J. Experimental study of hybrid FRP reinforced concrete beams. Engineering Structures. 2010. 32 (12). Pp. 3857–3865. DOI: 10.1016/j.engstruct.2010.08.028
22. Kara, I.F., Ashour, A.F., Köroğlu, M.A. Flexural behavior of hybrid FRP/steel reinforced concrete beams. Composite Structures. 2015. 129. Pp. 111–121. DOI: 10.1016/j.compstruct.2015.03.073
23. Dong, Z., Wu, G., Xu, Y. Experimental study on the bond durability between steel-FRP composite bars (SFCBs) and sea sand concrete in ocean environment. Construction and Building Materials. 2016. 115. Pp. 277–284. DOI: 10.1016/j.conbuildmat.2016.04.052
24. Lee, J.-Y., Lim, A.-R., Kim, J., Kim, J. Bond behaviour of GFRP bars in high-strength concrete: bar diameter effect. Magazine of Concrete Research. 2017. 69 (11). Pp. 541–554. DOI: 10.1680/jmacr.15.00403

25. Dong, Z., Wu, G., Xu, B., Wang, X., Taerwe, L. Bond performance of alkaline solution pre-exposed FRP bars with concrete. Magazine of Concrete Research. 2018. 70 (17). Pp. 894–904. DOI: 10.1680/jmacr.17.00027

26. Yang, Y., Wu, G. Evaluation of fatigue performance of ballastless track slabs reinforced with basalt-FRP and steel-FRP composite bars. Magazine of Concrete Research. 2020. 72 (1). Pp. 43–54. DOI: 10.1680/jmacr.18.00179

27. Chai, L., Guo, L., Chen, B., Ding, C. Bond behaviour of bars embedded in ecological high-ductility cementitious composites. Magazine of Concrete Research. 2020. 72 (3). Pp. 122–133. DOI: 10.1680/jmacr.18.00160

28. Bostel, R., Dos Santos, A.C.P., Lopes, J.B., Willrich, F.L., Hönnicke, M.G. Watching the bonding between steel rebar and concrete with in situ X-ray imaging. Magazine of Concrete Research. 2020. 72 (15). Pp. 768–777.

29. Sarapata, A., Ruiz-Yaniz, M., Zanette, I., Rack, A., Pfeiffer, F., Herzen, J. Multi-contrast 3D X-ray imaging of porous and composite materials. Applied Physics Letters. 2015. 106 (15). Pp. 154102. DOI: 10.1063/1.4918617

30. Clark, G.L., Smith, H.A. X-Ray Diffraction Study of Fractionated Paraffin Waxes. Industrial and Engineering Chemistry. 1931. 23 (6). Pp. 697–701. DOI: 10.1021/ie50258a025

31. Farrow, G. The measurement of crystallinity in polypropylene fibres by X-ray diffraction. Polymer. 1961. 2 (C). Pp. 409–417. DOI: 10.1016/0032-3861(61)90046-5

32. Wei, B., Cao, H., Song, S. Tensile behavior contrast of basalt and glass fibers after chemical treatment. Materials and Design. 2010. 31 (9). Pp. 4244–4250. DOI: 10.1016/j.matdes.2010.04.009

33. Tighiouart, B., Benmokrane, B., Gao, D. Investigation of bond in concrete member with fibre reinforced polymer (FRP) bars. Construction and Building Materials. 1998. 12 (8). Pp. 453–462. DOI: 10.1016/S0950-0618(98)00027-0

Information about authors:

Rudney Bostel,
ORCID: *https://orcid.org/0000-0003-4354-3040*
E-mail: *rudney.bostel@unila.edu.br*

Ana Carolina Parapinski dos Santos, D.Eng.
ORCID: *https://orcid.org/0000-0002-4359-8714*
E-mail: *ana.santos@unila.edu.br*

Joao Bernardino de Oliveira Lopes,
ORCID: *https://orcid.org/0000-0001-8370-0616*
E-mail: *joaobol@itaipu.gov.br*

Fabio Luiz Willrich,
ORCID: *https://orcid.org/0000-0003-0215-6044*
E-mail: *fabiolw@itaipu.gov.br*

Rodrigo Leonardo de Oliveira Basso, D.Sc.
ORCID: *https://orcid.org/0000-0001-9815-1592*
E-mail: *rodrigo.basso@unila.edu.br*

Marcelo Goncalves Honnicke, D.Sc.
ORCID: *https://orcid.org/0000-0003-3276-4323*
E-mail: *marcelo.honnicke@unila.edu.br*